

Large-Scale Hexagonal-Patterned Growth of Aligned ZnO Nanorods for Nano-optoelectronics and Nanosensor Arrays

Xudong Wang, Christopher J. Summers, and Zhong Lin Wang*

Center for Nanoscience and Nanotechnology, School of Materials Science and Engineering, Georgia Institute of Technology, Atlanta, Georgia 30332-0245

Received November 29, 2003; Revised Manuscript Received January 11, 2004

ABSTRACT

An effective approach is demonstrated for growing large-area, hexagonally patterned, aligned ZnO nanorods. The synthesis uses a catalyst template produced by a self-assembled monolayer of submicron spheres and guided vapor–liquid–solid (VLS) growth on a single crystal alumina substrate. The ZnO nanorods have uniform shape and length, align vertically on the substrate, and are distributed according to the pattern defined by the catalyst template. The nanorods grow along [0001] with side surfaces defined by $\{2\bar{1}\bar{1}0\}$. This approach opens the possibility of creating patterned one-dimensional nanostructures for applications as sensor arrays, piezoelectric antenna arrays, optoelectronic devices, and interconnects.

Quasi-one-dimensional (1D) zinc oxide,¹ a direct wide band gap (3.37 eV) semiconductor with a large excitation binding energy (60 meV), is one of the most important functional oxide nanostructures, exhibiting near-UV emission,² transparent conductivity, and piezoelectricity.³ The growth of patterned and aligned 1D ZnO nanostructures has huge promise for applications in sensing,⁴ optoelectronics,⁵ and field emission.^{6,7} Aligned growth of ZnO nanorods has been successfully achieved on a solid substrate via a vapor–liquid–solid (VLS) process, with the use of gold^{8,9} and tin¹⁰ as catalysts, in which the catalyst initiates and guides the growth, and the epitaxial orientation relationship between the nanorods and the substrate leads to the aligned growth. Other techniques that do not use any catalyst, such as metalorganic vapor-phase epitaxial growth,¹¹ template-assisted growth,⁶ and electrical field alignment,¹² have also been employed for the growth of vertically aligned ZnO nanorods. Recently, Kempa et al. have demonstrated a technique of growing periodically arranged carbon nanotubes using a catalyst pattern produced from a mask with the use of self-assembled submicron spheres.^{13,14} In this letter, we combine the self-assembly-based mask technique with the surface epitaxial approach to grow large-area hexagonal arrays of aligned ZnO nanorods. This approach opens the possibility of creating patterned 1D nanostructures for applications as sensor arrays, piezoelectric antenna arrays, optoelectronic devices, and interconnects.

The synthesis process involves three main steps. The hexagonally patterned ZnO nanorod arrays are grown onto a single-crystal Al₂O₃ substrate, on which patterned Au catalyst particles are dispersed. First, a two-dimensional, large-area, self-assembled and ordered monolayer of submicron spheres was formed on a single-crystal Al₂O₃ substrate. Second, a thin layer of gold particles was deposited onto the self-assembled monolayer; and then the spheres were etched away, leaving a patterned gold catalyst array. Finally, nanorods were grown on the substrate using a VLS process. Details on each step are described below.

Monolayer Self-Assembled Arrays of Submicron Spheres. The first step was to prepare an ordered monolayer of spheres by self-assembly. For this, monodispersed polystyrene (PS) spheres suspensions were purchased from Duke Scientific Corp. and used as received. The concentration of the suspensions was 10% spheres and the diameter of the spheres used in our experiments was 895 nm. For deposition, a 1 cm × 1 cm single-crystal sapphire ($2\bar{1}\bar{1}0$) substrate was sonicated for 20 min in a 2% Hellmanex II solution followed by a 3 h anneal in air at 1000 °C to achieve a completely hydrophilic and atomically flat surface. Then, 2 or 3 drops of the PS sphere suspension was applied to the surface of the substrate. After holding the substrate stationary for 1 min to obtain good dispersion of the suspension, the sapphire substrate was then slowly immersed into deionized water. Once the suspension contacted the water's surface, a monolayer of PS spheres was observed to immediately form, both

* Corresponding author. E-mail: zhong.wang@mse.gatech.edu.

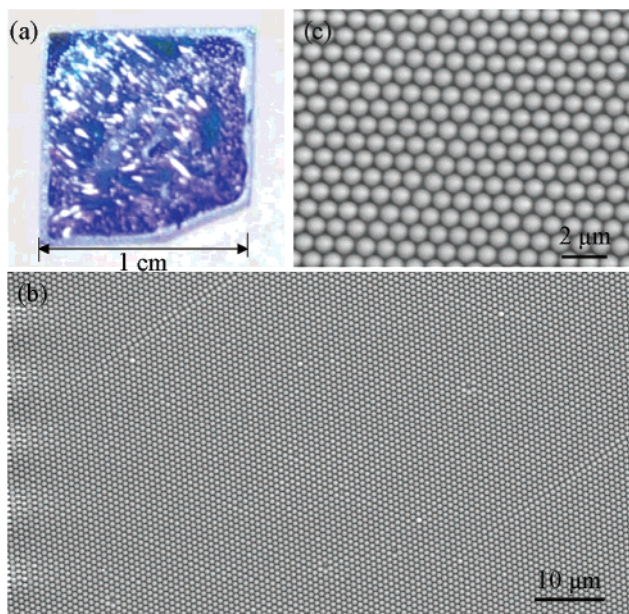


Figure 1. (a) Optical image of a monolayer of self-assembled polystyrene submicron spheres on an alumina substrate. (b, c) Low and high magnification SEM images, respectively, of a self-assembled monolayer of polystyrene spheres.

on the surface of the water and on the surface of the sapphire substrate. To prevent any further additions to the substrate it was kept immersed. Then, a few drops of 2% dodecylsodiumsulfate solution were added to the water to change the surface tension. As a result, the monolayer of PS spheres that remained suspended on the surface of the water was pushed aside due to the change in the surface tension. The substrate was then removed through the clear area where the surface tension of the water had been modified by the surfactant; thus, no additional PS spheres were deposited on the monolayer during its removal from the water. A metal frame was used to support the sample above the water surface while the sample was sonicated to avoid clustering of the PS spheres during drying.

Figure 1a shows an optical image of the self-assembled monolayer structure formed by this technique. The substrate was 90% covered by the monolayer while the different colors represent different domains of the monolayer, which were formed as a consequence of different orientations of the sphere arrays. The area of a single domain can reach a few square millimeters. The detailed organization of the spheres was investigated by scanning electron microscopy (SEM). Figure 1b is a low magnification SEM image, which shows a relatively large area of the self-assembled monolayer. The ordering is reasonably good although point defects and stacking faults are observed in some areas, which may be produced by a variation in sphere size. A closer examination presented in Figure 1c shows perfectly ordered arrays.

Preparation of Patterned Catalyst. The self-assembled arrays of PS spheres were then used to pattern the catalyst used to guide ZnO growth onto substrate. For this process, gold particles were either sputtered or thermally evaporated onto the self-assembled monolayer structure; as a result, two different patterns were obtained. For the sputtered coatings

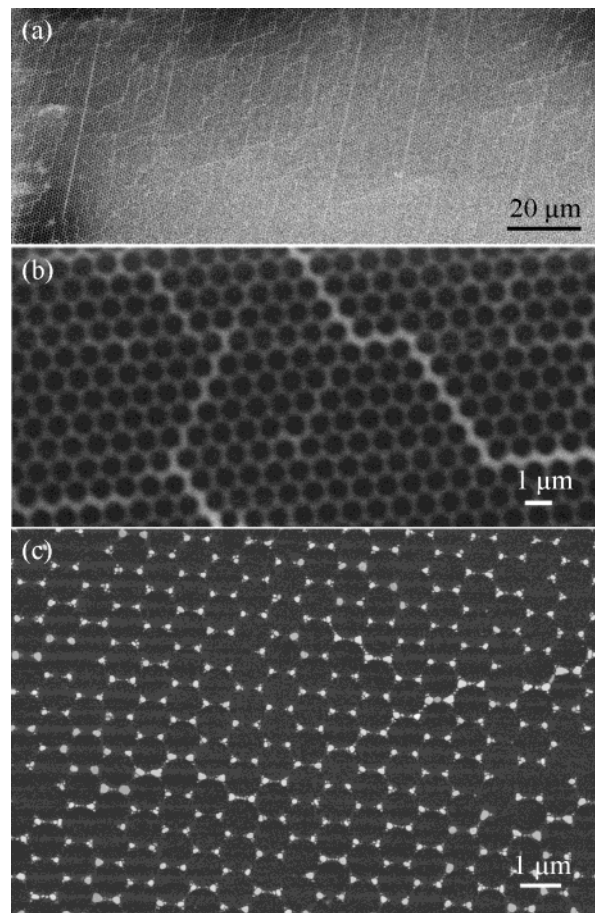


Figure 2. (a) Low magnification SEM image of a gold particle pattern deposited onto a substrate using the mask provided by a self-assembled monolayer of polystyrene spheres; (b) high magnification of the pattern, showing the honeycomb pattern produced by a sputtering technique. (c) Gold pattern produced by an evaporation technique using the shadow provided by the monolayer of self-assembled polystyrene spheres.

the high mobility of the gold atoms during the sputtering process, resulted in gold covering every available area, even beneath the spheres. Therefore, after etching away the PS spheres using toluene, this technique produced a honeycomb-like hexagonal gold pattern, as shown by the SEM images in Figure 2a and 2b. However, by using a thermal evaporator, which provides a line of sight vapor stream, the gold particles were only deposited onto areas of the substrate that were not shadowed by the PS spheres. After etching away the PS spheres, a highly ordered hexagonal array of gold spots was formed on the substrate (Figure 2c).

Growth of Patterned ZnO Nanorod Arrays. Using the patterned catalyst, ZnO nanorods were grown by a solid-liquid-vapor process. The source materials contained equal amounts (by weight) of ZnO powder (0.8 g) and graphite powder, which was used to lower the growth temperature. The source materials were then ground together and loaded into an alumina boat that was placed at the center of an alumina tube with the substrate being positioned slightly downstream from the tube's center. Both ends of the tube were water cooled to achieve a reasonable temperature gradient. A horizontal tube furnace was used to heat the tube

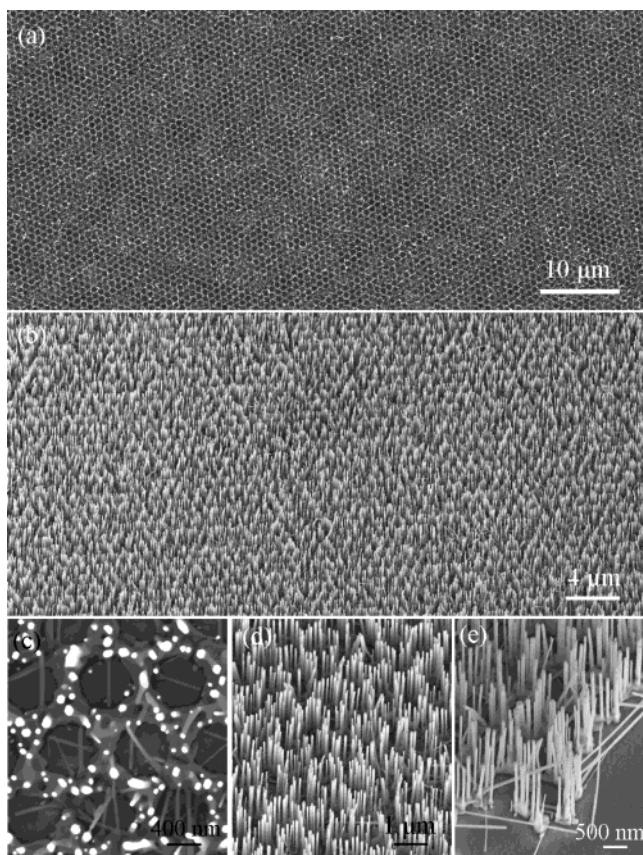


Figure 3. (a) Low magnification top-view SEM image of aligned ZnO nanorods grown onto a honeycomb catalyst pattern as shown in Figure 2a. (b) Side view of the aligned ZnO nanorods at an angle of 30°. (c, d) Top and a 30° view of aligned ZnO nanorods, where the hexagonal pattern is apparent. (d) Aligned ZnO nanorods at the edge of the growth pattern.

to 950 °C at a rate of 50 °C/min, and the temperature was held for 20–30 min under a pressure of 300–400 mbar at a constant argon flow at 25 sccm. Then the furnace was shut down and cooled to room temperature under a flow of argon.

Figure 3 presents SEM images recorded from the ZnO nanorod arrays. Figure 3a shows a top view of the ZnO nanorod arrays over a large area. It is clear that the honeycomb-like arrangement of the gold pattern was preserved during the growth process. A magnified image of the top view is shown in Figure 3c. Each white spot represents one ZnO nanorod oriented perpendicular to the sapphire substrate and at the tip is a gold particle. Some ZnO nanorods that grew sideways were also observed. A 30° side view of the arrays (Figure 3b) shows clearly the well-aligned growth of the ZnO nanorods. The hexagonal arrangement of the aligned ZnO nanorods can be clearly distinguished in the magnified image shown in Figure 3d. All of the ZnO nanorods have about the same height, of about 1.5 μm and their diameters range between 50 and 150 nm. By changing the growth time the height of the ZnO nanorods could be varied from a few hundred nanometers to a few micrometers. Figure 3e is a higher magnification SEM image taken at the edge of an array. It clearly demonstrates that most of the ZnO nanorods grow perpendicular to the substrate (that is, vertically), but that a few can also grow parallel to the

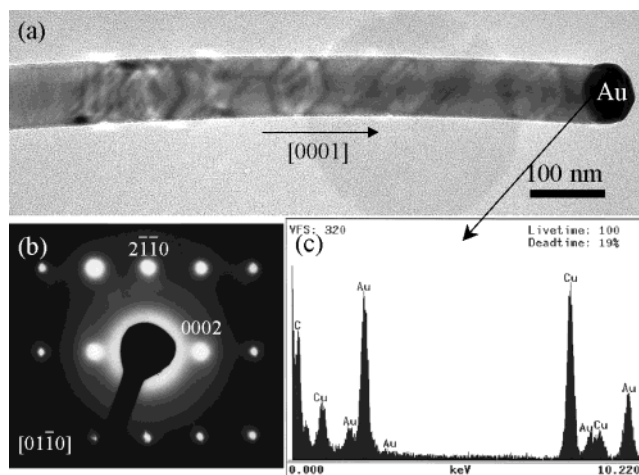


Figure 4. (a) TEM image of a ZnO nanorod with an Au particle at the end. (b) Electron diffraction pattern of a nanorod. (c) EDS spectrum recorded from the catalyst particle.

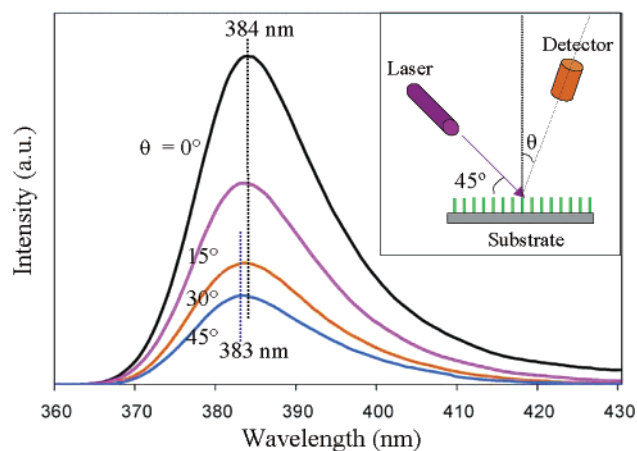


Figure 5. Photoluminescence (PL) spectra acquired from an aligned ZnO nanorod array as a function of the angle between the detector and a direction normal to the substrate. The inset shows the experimental set up.

substrate, and have a growth root from the same catalyst particle that promotes vertical nanorod growth.

Transmission electron microscopy (TEM) was used to characterize the crystallography of the ZnO nanorods. Figure 4a shows a ZnO nanorod with a catalyst particle at the tip. The contrast observed along the length of the nanorod displays the hexagonal cross section of the ZnO nanorod. An electron diffraction pattern recorded from a nanorod indicates that the nanorod grows along [0001] and its side surfaces are defined by $\{2\bar{1}10\}$ (Figure 4b). The tip of the nanorod was confirmed to be a gold particle from energy-dispersive X-ray spectroscopy (EDS) (Figure 4c), where the copper and carbon signatures are from the copper TEM grid coated with a carbon film.

Photoluminescence (PL) spectra were acquired from the aligned ZnO nanorods to reveal their collective optical properties. The PL measurements were performed at room temperature using a 337 nm N₂ pulsed laser as the excitation light source. The laser pulse frequency was 15 Hz, with 800 ps pulse duration at an average energy of 50 mW. The laser

was incident onto the sample at an angle of 45°, while the detection angle was defined as the angle between the detector and the direction normal to the substrate, as shown in the inset in Figure 5. The emission spectra were recorded at four different detection angles, 0, 15, 30, and 45 degrees (Figure 5). Unlike the data that we reported previously for other types of 1D ZnO nanobelt¹⁵ and nanorod¹⁶ geometries, all of which had a luminescence peak at 387 nm, the aligned ZnO nanorods exhibit a peak at 384 nm at $\theta = 0$ degree. As the detection angle was increased, the luminescence intensity dropped dramatically, which may indicate that the luminescence was emitted mainly along the axis of the ZnO nanorods. Moreover, the luminescence peak shifted very slightly from 384 to 383 nm when the detection angle increased from 0 to 45 degrees. This may also be caused by the polarization of the emitted light from the aligned nanorods.¹⁷

In summary, we have presented an effective approach for growing large-area, patterned, aligned ZnO nanorods. The synthesis technique uses a catalyst template produced from a self-assembled monolayer of submicron polystyrene spheres that guides the VLS growth of ZnO onto a single-crystal alumina substrate. This approach opens the possibility of creating patterned 1D nanostructures for applications as sensor arrays, piezoelectric antenna arrays, optoelectronic devices, and interconnects.

Acknowledgment. We are thankful for financial support from a US NSF grant DMR-9733160 and the MURI program for ARO grant DAAD19-01-1-0603.

References

- (1) *Nanowires and Nanobelts, Vol. I: Metal and Semiconductor Nanowires*, and *Vol. II: Nanowire and Nanobelt of Functional Oxide*; Wang Z. L., Ed.; Kluwer Academic Publisher: Norwell, MA, 2003.
- (2) Service, R. F. *Science* **1997**, *276*, 895.
- (3) Kong, X. Y.; Wang, Z. L. *Nano Lett.* **2003**, *3*, 1625.
- (4) Arnold, M. S.; Avouris, Ph.; Pan, Z. W.; Wang, Z. L. *J. Phys. Chem. B* **2003**, *107*, 659.
- (5) Huang, M. H.; Mao, S.; Feick, H.; Yan, H.; Wu, Y.; Kind, H.; Weber, E.; Russo, R.; Yang, P. *Science* **2001**, *292*, 1897.
- (6) Liu, C.; Zapien, J. A.; Yao, Y.; Meng, X.; Lee, C. S.; Fan, S.; Lifshitz, Y.; Lee, S. T. *Adv. Mater.* **2003**, *15*, 838.
- (7) Bai, X. D.; Wang, E. G.; Gao, P. X.; Wang, Z. L. *Nano Lett.* **2003**, *3*, 1147.
- (8) Ng, H. T.; Chen, B.; Li, J.; Han, J.; Meyyappan, M.; Wu, J.; Li, X.; Haller, E. E. *Appl. Phys. Lett.* **2003**, *82*, 2023.
- (9) Zhao, Q. X.; Willander, M.; Morjan, R. R.; Hu, Q. H.; Campbell, E. E. *Appl. Phys. Lett.* **2003**, *83*, 165.
- (10) Gao, P. X.; Ding, Y.; Wang, Z. L. *Nano Lett.* **2003**, *3*, 1315.
- (11) Park, W. I.; Kim, D. H.; Jung, S. W.; Yi, G. C. *Appl. Phys. Lett.* **2002**, *80*, 4232.
- (12) Harnack, O.; Pacholski, C.; Weller, H.; Yasuda, A.; Wessels, J. M. *Nano Lett.* **2003**, *3*, 1097.
- (13) Kempa, K.; Kimball, B.; Rybczynski, J.; Huang, Z. P.; Wu, P. F.; Steeves, D.; Sennett, M.; Giersig, M.; Rao, D. V. G. L. N.; Carnahan, D. L.; Wang, D. Z.; Lao, J. Y.; Li, W. Z.; Ren, Z. F. *Nano Lett.* **2003**, *3*, 13.
- (14) Huang, Z. P.; Carnahan, D. L.; Rybczynski, J.; Giersig, M.; Sennett, M.; Wang, D. Z.; Wen, J. G.; Kempa, K.; Ren, Z. F. *Appl. Phys. Lett.* **2003**, *82*, 460.
- (15) Wang, X. D.; Gao, P. X.; Li, J.; Summers, C. J.; Wang, Z. L. *Adv. Mater.* **2002**, *14*, 1732.
- (16) Wang, X. D.; Summers, C. J.; Wang, Z. L. *Adv. Mater.* **2003**, submitted.
- (17) Johnson, J. C.; Yan, H.; Yang, P. Saykally, R. J. *J. Phys. Chem. B* **2003**, *107*, 8816.

NL035102C